



HAL
open science

Rotating magnetoconvection with anisotropic diffusivities in the Earth's core

Tomas Soltis

► **To cite this version:**

Tomas Soltis. Rotating magnetoconvection with anisotropic diffusivities in the Earth's core. *Physics of the Earth and Planetary Interiors*, 2009, 178 (1-2), pp.27. 10.1016/j.pepi.2009.08.013 . hal-00601521

HAL Id: hal-00601521

<https://hal.science/hal-00601521>

Submitted on 18 Jun 2011

HAL is a multi-disciplinary open access archive for the deposit and dissemination of scientific research documents, whether they are published or not. The documents may come from teaching and research institutions in France or abroad, or from public or private research centers.

L'archive ouverte pluridisciplinaire **HAL**, est destinée au dépôt et à la diffusion de documents scientifiques de niveau recherche, publiés ou non, émanant des établissements d'enseignement et de recherche français ou étrangers, des laboratoires publics ou privés.

Accepted Manuscript

Title: Rotating magnetoconvection with anisotropic diffusivities in the Earth's core

Author: Tomas Soltis

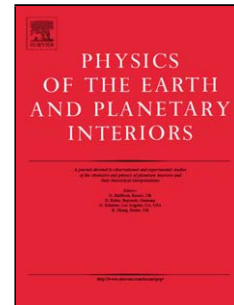
PII: S0031-9201(09)00194-0
DOI: doi:10.1016/j.pepi.2009.08.013
Reference: PEPI 5202

To appear in: *Physics of the Earth and Planetary Interiors*

Received date: 10-1-2009
Revised date: 1-6-2009
Accepted date: 31-8-2009

Please cite this article as: Soltis, T., Rotating magnetoconvection with anisotropic diffusivities in the Earth's core, *Physics of the Earth and Planetary Interiors* (2008), doi:10.1016/j.pepi.2009.08.013

This is a PDF file of an unedited manuscript that has been accepted for publication. As a service to our customers we are providing this early version of the manuscript. The manuscript will undergo copyediting, typesetting, and review of the resulting proof before it is published in its final form. Please note that during the production process errors may be discovered which could affect the content, and all legal disclaimers that apply to the journal pertain.



1 Introduction

The topic of the presented paper is marginally related to two interesting and open problems – turbulence and the dynamo paradox. Turbulence is still considered to be one of the most challenging and not yet resolved problems. The geodynamo paradox is related to the Earth’s core, in which the flows, very probably turbulent, generate and sustain the main geomagnetic field through the dynamo process. Very recently computer simulations of the geodynamo have provided models of the geomagnetic field, which give a true picture with all significant features of the observed field with its secular variations.

The paradox lies in the fact, that due to the computer limitations unrealistically high diffusion coefficients (for example viscosity) were used. Even accepting the turbulent viscosity and other diffusivities of the Earth’s core, the values used in those models were noticeably higher. Thus, it was necessary to introduce hyperviscosity into the simulations to reach agreement between the observed and simulated fields. It means also that formally some type of anisotropy of diffusive coefficients was considered.

We study the conditions for marginal convection in the horizontal planar layer rotating about a vertical axis permeated by a homogeneous horizontal magnetic field. It is a model employed in [5, 6, 13, 9], which studied both the stationary convection and the periodic instability of modes in the form of rolls inclined to the magnetic field. Considering also the case of isotropic diffusion we have advanced these studies by including two types of anisotropic diffusive coefficients. We christened the first type stratification anisotropy (SA) and it is a crude analogue of hyperdiffusivities used in computer simulations. We distinguished the diffusivities in the vertical direction from horizontal diffusivities (which are considered to be horizontally isotropic) and we introduced two sub-cases: oceanic type of SA and the atmospheric type of SA , respectively. In the first one (oceanic), the diffusivities in the horizontal directions are greater than in the vertical one. In the second sub-case (atmospheric) it is the reverse. The second type of anisotropy is analogous to the result obtained in [1] and it is given by the directions of the basic magnetic field, \mathbf{B} , and the rotation, $\mathbf{\Omega}$. In the direction of $\mathbf{\Omega} \times \mathbf{B}$ the diffusivities are much smaller than in the directions of $\mathbf{\Omega}$ and \mathbf{B} .

We focus our attention on the special type of instabilities which are affected by diffusive processes. Of course, we can expect that these diffusive instabilities, in particular, will be strongly influenced by anisotropic diffusive coefficients. Especially, if one reminds oneself that the conventional understanding of the role of diffusion — only weak damping of the instabilities which arise — is not sufficient. It is generally accepted, that the dynamics of the Earth’s core are determined by three basic forces: magnetic, Archimedean and Coriolis forces (\mathbf{M} , \mathbf{A} , and \mathbf{C} , respectively). However, diffusive processes may weaken the basic forces in the sense: viscosity weakens only the Coriolis force, magnetic diffusivity weakens only the magnetic force, and thermal diffusivity weakens only the Archimedean force and a new triad of basic forces, $\mathbf{M} - \delta\mathbf{M}$, $\mathbf{A} - \delta\mathbf{A}$, and $\mathbf{C} - \delta\mathbf{C}$, develops completely new balance of forces prone to new and even

unexpected instabilities.

The present paper extends the papers [5, 6, 13, 9], where the diffusive coefficients were isotropic. The paper continues in our strategy to modify old models or to set up new models of linear rotating magnetoconvection in the sense of introducing anisotropic diffusive coefficients. For instance, the results of our models of horizontal planar layer of fluid with other basic magnetic fields (homogeneous vertical or non-homogeneous azimuthal, see e.g. [2]) or with non-vertical orientation of rotation axis are upcoming for publication. We consider the horizontal magnetic field and vertical rotation axis, chosen in this paper, as a crude approximation of the Earth's azimuthal magnetic field in polar regions (not too close to poles). On the other hand, the equatorial region can be approximated by the horizontal planar fluid layer permeated by horizontal magnetic field but rotating about horizontal axis perpendicular to the field.

The results are in the form of conditions for the onset of instabilities which are set by new parameters — parameters of anisotropy of diffusive coefficients. In the case of turbulent transport phenomena the shape of transporters, i.e. eddies, distinguish transport efficiency in various directions. For that reason it is convenient to change the isotropic transport phenomena, usual in the molecular case, into the anisotropic ones. It means: for transport coefficients we have the transition from scalar into tensor quantities. Recent surveys of problems related to the Earth's core turbulence, the geodynamo paradox and some models of the geodynamo and rotating magnetoconvection with anisotropic diffusive coefficients are in [7, 14, 8], where it is possible to find some important references, too.

The structure of the paper is the following: after definitions of the two types of considered anisotropies (Sect. 2), the mathematical formulation is stated and the basic dispersion relation for the two anisotropic cases is derived (Sect. 3). The method of solution for steady and overstable convection is described in Sect. 4. The influence of anisotropy on steady modes is described and numerical results are discussed in Sect. 5. Overstable modes in anisotropic cases are described in Sect. 6. The most important results are summarized and the paper is concluded in Sect. 7.

2 Anisotropy of diffusive coefficients

We introduce possibly the simplest forms of anisotropy, in which the thermal diffusion and viscosity are considered¹ to be in the form of a diagonal Cartesian tensor with only two different values of its 3 components

$$\boldsymbol{\nu} = \begin{pmatrix} \nu_{xx} & 0 & 0 \\ 0 & \nu_{yy} & 0 \\ 0 & 0 & \nu_{zz} \end{pmatrix}.$$

¹see expressions (8, 9) and (10) for anisotropic Laplacian ∇_{α}^2 in equations (3) and (5), respectively.

It means that in two directions the diffusion is the same, but different from the diffusion in the third direction. For instance $\nu_{xx} = \nu_{yy} \neq \nu_{zz}$ or $\nu_{xx} \neq \nu_{yy} = \nu_{zz}$. We consider two basic types of anisotropy (*SA* and *BM*) of diffusive processes in the models investigated in this paper. The definitions of *SA* or *BM* type anisotropy (stratification anisotropy or Braginsky-Meytlis anisotropy) depend on the importance of basic forces determining the dynamics of the system. However, both anisotropy types *SA* and *BM*, can be formally determined by single value of diffusive coefficient, e.g. by vertical component ν_{zz} or κ_{zz} and by the anisotropy parameter, α .

We define the parameter of anisotropy α , a measure of anisotropy, as the ratio of two considered values of diffusivity in two different directions. Thus a measure of the anisotropy of viscosity is the parameter, $\alpha_\nu = \nu_{xx}/\nu_{zz}$. Analogously, a measure of the anisotropy of thermal diffusivity is the parameter, $\alpha_\vartheta = \kappa_{xx}/\kappa_{zz}$. Henceforth, we will assume that these parameters are equal,

$$\alpha \equiv \alpha_\nu = \frac{\nu_{xx}}{\nu_{zz}} = \alpha_\vartheta = \frac{\kappa_{xx}}{\kappa_{zz}}, \quad (1)$$

and different subscripting, if it is used, will be only for lucidity and for realising the connection between the parameters and the physical processes.

2.1 *SA*, Stratification anisotropy

In the *SA* case the density stratification determined by the vertical direction of gravity or/and the Archimedean buoyancy force has dominant influence on the dynamics of eddies. The axis of rotation has also the vertical direction z . We christen this type of anisotropy as stratification anisotropy (*SA*). The anisotropy is defined in the sense that diffusive coefficients have different values in the vertical direction z than in the horizontal directions x and y . We distinguish two types of this anisotropy depending on the fact that the diffusivity in the vertical direction can be greater or smaller in comparison with diffusivity in the horizontal directions (in the horizontal directions we consider isotropic diffusion, i.e. diffusion is the same in all directions of the horizontal plane, e.g. for viscosity $\nu_{xx} = \nu_{yy}$). If the diffusivity in the vertical direction is greater than in the horizontal directions, we christen it *a*-anisotropy, which is a rough analogue of the lowermost part of the atmosphere in which turbulent transport in the vertical direction is facilitated by the developed convection. This atmospheric type of *SA* anisotropy is thus defined: $\nu_{zz} > \nu_{xx} = \nu_{yy}$ and $\kappa_{zz} > \kappa_{xx} = \kappa_{yy}$, and the parameter (1) of anisotropy, α , has values less than one. If the opposite case is considered, it means that the diffusivity is smaller in the vertical direction than in the horizontal directions; we call it *o*-anisotropy, i.e. oceanic *SA* anisotropy, which is analogous to the uppermost layer of the ocean, stably stratified during the day due to the heating from above. The consequence is the weakened turbulent transport in the vertical direction. In this case the anisotropy is defined by $\nu_{zz} < \nu_{xx} = \nu_{yy}$ and $\kappa_{zz} < \kappa_{xx} = \kappa_{yy}$, with the anisotropy parameter α greater than one (1).

2.2 *BM*, Braginsky and Meytlis type anisotropy

If rotation and the magnetic field have the dominant influence on the dynamics of turbulent eddies, we can suppose *BM* type anisotropy (from the study by Braginsky and Meytlis [1] of local turbulence in the Earth's core) of the system, in which the diffusive coefficients are greater in the direction of rotation (in the vertical direction) z and in the y direction of magnetic field (we suppose a homogeneous magnetic field in the horizontal direction y), than the diffusivities in the third direction x . *BM* type anisotropy is defined subsequently: $\nu_{zz} = \nu_{yy} > \nu_{xx}$ and $\kappa_{zz} = \kappa_{yy} > \kappa_{xx}$. The parameter (1) of anisotropy α is smaller than one in this case. In cylindrical coordinates the anisotropy results in the relationships, $\nu_{zz} \sim \nu_{\varphi\varphi} \gg \nu_{ss}$ and $\kappa_{zz} \sim \kappa_{\varphi\varphi} \gg \kappa_{ss}$, [1].

Some codes for each investigated type of anisotropy are used. Individual types of anisotropies are coded by their physical background which determine the range of anisotropy parameter values, α , too.

- SA* \Rightarrow stratification anisotropy, $\nu_{xx} = \nu_{yy} \neq \nu_{zz}$, $0 < \alpha < 1$ or $\alpha > 1$
- Sa* \Rightarrow *SA* anisotropy of atmospheric type, *a* type of *SA* anisotropy, $0 < \alpha < 1$
- So* \Rightarrow *SA* anisotropy of oceanic type, *o* type of *SA* anisotropy, $\alpha > 1$
- BM* \Rightarrow Braginsky and Meytlis type anisotropy, $\nu_{xx} \neq \nu_{yy} = \nu_{zz}$, $0 < \alpha < 1$

3 Model

Linear stability of the infinite horizontal plane layer of incompressible fluid and of the width, d , is examined. The layer is permeated by homogeneous horizontal magnetic field, \mathbf{B}_0 , in the y direction, rotates about a vertical axis z , and gravity, \mathbf{g} , is in the $-z$ direction. The layer is heated from below and cooled from above. Thus the linear profile of the temperature, T_0 , is sustained; see Fig. 1.

We try to choose the parameters of the layer including diffusive coefficients so that they can correspond to the Earth's core. Therefore, we suppose that values of viscosity and thermal diffusivity are determined by turbulent eddies strongly shaped by basic forces in the core. Due to metallic electric conductivity, σ , of the Earth's core there is a good reason [7, 8, 14] to neglect the turbulent contribution to the value of the magnetic diffusivity, $\eta = 1/\mu_0\sigma$ (μ_0 is magnetic permeability). Thus η in our models is isotropic. However, our study is focused on the influence of anisotropic diffusive coefficients (coefficients of viscosity and thermal diffusivity) on the onset of thermally driven instabilities, i.e. the influence of anisotropy (1) parameter α in the *SA* and *BM* cases on rotating magnetoconvection in the form of horizontally oriented rolls.

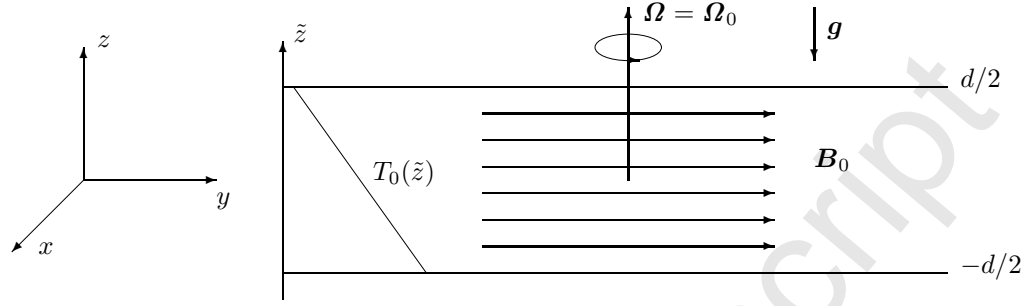


Figure 1: Model of rotating magnetoconvection with homogeneous horizontal basic magnetic field in the infinite horizontal unstable stratified fluid layer with temperature profile, $T_0(\tilde{z})$.

3.1 Basic equations

We consider the basic state of the system (rotating with angular velocity, $\boldsymbol{\Omega}_0 = \Omega_0 \hat{\mathbf{z}}$),

$$\mathbf{U}_0 = \mathbf{0}, \quad \mathbf{B}_0 = B_M \hat{\mathbf{y}}, \quad T_0 = T_l - \Delta T \frac{\tilde{z} + d/2}{d}, \quad (2)$$

where $\hat{\mathbf{y}}$ and $\hat{\mathbf{z}}$ are unit vectors in directions y and z , respectively. T_l is a basic temperature at the bottom of the layer, $\tilde{z} = -d/2$, and ΔT is the basic temperature difference between the top and the bottom of the layer. We investigate the system stability by putting perturbations of the velocity field, magnetic field and temperature, $\tilde{\mathbf{u}}$, $\tilde{\mathbf{b}}$ and $\tilde{\vartheta}$, respectively, into the system of basic equations. This system for the unknown perturbations is converted into the dimensionless and linearized form,

$$R_o \frac{\partial \mathbf{u}}{\partial t} + \hat{\mathbf{z}} \times \mathbf{u} = -\nabla p + \Lambda (\nabla \times \mathbf{b}) \times \hat{\mathbf{y}} + R \vartheta \hat{\mathbf{z}} + E_z \nabla_\alpha^2 \mathbf{u}, \quad (3)$$

$$\frac{\partial \mathbf{b}}{\partial t} = \nabla \times (\mathbf{u} \times \hat{\mathbf{y}}) + \nabla^2 \mathbf{b}, \quad (4)$$

$$\frac{1}{q_z} \frac{\partial \vartheta}{\partial t} = \hat{\mathbf{z}} \cdot \mathbf{u} + \nabla_\alpha^2 \vartheta, \quad (5)$$

$$\nabla \cdot \mathbf{u} = 0, \quad (6)$$

$$\text{and } \nabla \cdot \mathbf{b} = 0, \quad (7)$$

using the following substitutions²,

$$\tilde{z} = dz, \quad \tilde{t} = \frac{d^2}{\eta}t, \quad \tilde{\mathbf{u}} = \frac{\eta}{d}\mathbf{u}, \quad \tilde{p} = 2\Omega_0\eta\rho_0p, \quad \tilde{\mathbf{b}} = B_M\mathbf{b}, \quad \tilde{\vartheta} = \frac{\eta\Delta T}{\kappa_{zz}}\vartheta,$$

where tilded symbols are quantities with dimension and nontilded symbols are their dimensionless counterparts. In the subsequent text only dimensionless quantities are used. ρ_0 and p are density and pressure (with contribution from the centrifugal force), respectively. At first glance one can see in (3) and (5) that the Laplacian ∇^2 is replaced by the anisotropic Laplacian ∇_α^2 ; see (8–10). The first equation (3) is the momentum Navier-Stokes equation, which describes the temporal behaviour of the perturbation velocity field \mathbf{u} . The second equation (4) is the induction equation describing the temporal behaviour of the perturbation magnetic field \mathbf{b} . The next equation of heat conduction (5) describes the behaviour of the temperature field perturbation ϑ in time. The last two equations express that the magnetic and velocity fields are solenoidal. In the Navier-Stokes equation we consider two forms of last term, $E_z\nabla_\alpha^2\mathbf{u}$, describing the viscous force, since we consider two types of anisotropy. In the case of stratification anisotropy (*SA*) the viscous term has the form,

$$E_z\nabla_\alpha^2\mathbf{u} = E_z[(1 - \alpha_\nu)\partial_{zz} + \alpha_\nu\nabla^2]\mathbf{u}, \quad (8)$$

and in the case of anisotropy by Braginsky and Meytlis (*BM*) the viscous term has the form,

$$E_z\nabla_\alpha^2\mathbf{u} = E_z[(\alpha_\nu - 1)\partial_{xx} + \nabla^2]\mathbf{u}. \quad (9)$$

In addition to the anisotropic coefficient of viscosity we suppose the anisotropy of thermal diffusion, too. In the equation of heat conduction we consider, therefore, two forms of the diffusive term $\nabla_\alpha^2\vartheta$. In *SA* and *BM* type anisotropy, respectively, the forms of diffusive terms are the following,

$$\nabla_\alpha^2\vartheta = [(1 - \alpha_\vartheta)\partial_{zz} + \alpha_\vartheta\nabla^2]\vartheta \quad \text{and} \quad \nabla_\alpha^2\vartheta = [(\alpha_\vartheta - 1)\partial_{xx} + \nabla^2]\vartheta. \quad (10)$$

We can easily prove in both cases of anisotropy, that setting the anisotropy parameters α_ν and α_ϑ to one (supposing isotropic diffusivities $\alpha = \alpha_\nu = \alpha_\vartheta = 1$), the diffusive terms in equations (3, 5) change into the commonly used forms, $E\nabla^2\mathbf{u}$ and $\nabla^2\vartheta$, respectively. Thus the greater α differs from one, the greater the anisotropy. We use dimensionless parameters expressing the ratio of quantities with equal dimension, for example ratios of individual forces or time scales or length scales, i.e.

$$R_o = \frac{\eta}{2\Omega_0d^2}, \quad A = \frac{B_M^2}{2\Omega_0\rho_0\mu\eta}, \quad E_z = \frac{\nu_{zz}}{2\Omega_0d^2}, \quad R = \frac{\alpha_Tg\Delta Td}{2\Omega_0\kappa_{zz}}, \quad q_z = \frac{\kappa_{zz}}{\eta} \quad (11)$$

²The special form of the scaling of the temperature perturbation $\tilde{\vartheta} = \frac{\eta\Delta T}{\kappa_{zz}}\vartheta$ is used for the modified Rayleigh number and equation of heat conduction in their commonly used forms. By using the simpler scaling, $\tilde{\vartheta} = \Delta T\vartheta$, the modified Rayleigh number has a form $R = \alpha_Tg\Delta Td/2\Omega_0\eta$ and the equation of heat conduction is then $\frac{1}{q_z}\frac{\partial\tilde{\vartheta}}{\partial t} = \frac{1}{q_z}\tilde{\mathbf{z}} \cdot \mathbf{u} + \nabla_\alpha^2\tilde{\vartheta}$.

where

R_o – the modified Rossby number is a ratio of rotation period to magnetic diffusion time (the classical Rossby number $R_o = U/\Omega_0 d$ is a measure of the ratio of rotation period to the time d/U , in which the characteristic flow in the system with the velocity U passes the characteristic length of the system, d);

A – the Elsasser number is a ratio of magnetic force and Coriolis force;

E_z – the Ekman number is a measure of viscous forces to Coriolis force. Due to anisotropic viscosity we have also the second Ekman number, $E_x = \nu_{xx}/2\Omega_0 d^2$;

R – the modified Rayleigh number measures effective buoyancy force to Coriolis force (where α_T is thermal expansion coefficient);

q_z – the Roberts number is defined as the ratio of magnetic and thermal diffusion time scales, i.e. the ratio of coefficients of thermal diffusion and magnetic diffusion. Similarly, as in the case of the Ekman number, the Roberts number has two different values, because we consider anisotropy of thermal diffusion. Thus we have the second Roberts number, $q_x = \kappa_{xx}/\eta$.

It is also useful to introduce five further dimensionless numbers

$$\zeta = \frac{\eta}{\kappa_{zz}} = q_z^{-1}, \quad p = \frac{\eta}{\nu_{zz}} = \frac{R_o}{E_z}, \quad Q = \frac{\Lambda}{E_z}, \quad T_a = E_z^{-2}, \quad R_a = \frac{R}{E_z}, \quad (12)$$

where ζ and p are two Prandtl numbers, dimensionless ratios of diffusivities, ζ – the inverse Roberts, and p – the inverse magnetic Prandtl number³. The next three numbers, Q – the Chandrasekhar, T_a – the Taylor, and R_a – the classical Rayleigh number are useful for comparison between corresponding formulas here and in [3, 5, 6].

4 Method of solution

In the following proceeding we split the perturbations of the velocity field \mathbf{u} and magnetic field \mathbf{b} into poloidal and toroidal parts,

$$\mathbf{u} = a^{-2} [\nabla \times (\nabla \times w \hat{\mathbf{z}}) + \nabla \times \omega \hat{\mathbf{z}}] \quad \text{and} \quad \mathbf{b} = a^{-2} [\nabla \times (\nabla \times b \hat{\mathbf{z}}) + \nabla \times j \hat{\mathbf{z}}]. \quad (13)$$

All perturbations (w , ω , b , j , and ϑ) have the form,

$$f(x, y, z, t) = \Re e [F(z) \exp(ilx + imy) \exp(\lambda t)], \quad (14)$$

where the horizontal components of the wave vector, l and m , determine $a^2 = l^2 + m^2$. The square root of a^2 is the horizontal wave number, a , and λ is a complex frequency ($\lambda = i\sigma$). The properties of convection dependent on the values l , m , and σ are discussed in the subsection 4.1.

Taking the z -components of the curl and double curl of the Navier-Stokes equation, the curl of the induction equation and the induction equation itself and the equation of heat conduction and substituting the perturbations (w , ω , b , j

³Due to the next ignoring of pressure we use symbol p for the one frequently used dimensionless number, $p = p_z$.

and ϑ) into these equations we obtain following set of ordinary differential equations for the unknown functions $F(z) = W(z)$, $\Omega(z)$, $B(z)$, $J(z)$, and $\Theta(z)$,

$$[E_z \mathcal{D}_\alpha - R_o \lambda] \Omega + DW + im\Lambda J = 0, \quad (15)$$

$$(D^2 - a^2) [E_z \mathcal{D}_\alpha - R_o \lambda] W - D\Omega + im\Lambda(D^2 - a^2)B = a^2 R\Theta, \quad (16)$$

$$(D^2 - a^2 - \lambda)J + im\Omega = 0, \quad (17)$$

$$(D^2 - a^2 - \lambda)B + imW = 0, \quad (18)$$

$$(\mathcal{D}_\alpha - \zeta\lambda)\Theta + W = 0, \quad (19)$$

where $D = d/dz$ and the operator \mathcal{D}_α has two different forms, that is $D^2 - \alpha l^2 - m^2$ and $D^2 - \alpha l^2 - \alpha m^2$ in *BM* and *SA* type anisotropy, respectively. From these five equations (15–19) we successively eliminate 4 unknown functions except W and we get an ordinary differential equation of the 12th order for W of the following form,

$$\begin{aligned} & \left[(\mathcal{D}_\alpha - \zeta\lambda) \left((D^2 - a^2) \{ \mathcal{D}_\lambda (\mathcal{D}_\alpha - p\lambda) + Qm^2 \}^2 + T_a \mathcal{D}_\lambda^2 D^2 \right) + \right. \\ & \left. + a^2 R_a \mathcal{D}_\lambda \{ \mathcal{D}_\lambda (\mathcal{D}_\alpha - p\lambda) + Qm^2 \} \right] W = 0, \end{aligned} \quad (20)$$

where $\mathcal{D}_\lambda = D^2 - a^2 - \lambda$ and the set of dimensionless parameters (11) was replaced by the set (12).

For direct comparison with [3] and [5, 6] we introduce also the substitutions,

$$\tilde{l} = \frac{l^2}{\pi^2}, \quad \tilde{m} = \frac{m^2}{\pi^2}, \quad \sigma_1 = -\frac{i\lambda}{\pi^2}, \quad T_1 = \frac{T_a}{\pi^4}, \quad Q_1 = \frac{Q}{\pi^2} \quad \text{and} \quad R_1 = \frac{R_a}{\pi^4}. \quad (21a)$$

If we consider the simplest boundary conditions at $z = -1/2, 1/2$ (in [13] christened illustrative conditions), i.e. the stress-free and perfect thermally and electrically conducting boundaries,

$$W = D^2 W = D\Omega = \Theta = B = DJ = 0,$$

then due to the solution $W = W_0 \cos(\pi z)$ we can replace the operators in (20) by simple algebraic formulas. Finally, introducing the auxiliary variables,

$$\tilde{a} = \tilde{l} + \tilde{m}, \quad A = 1 + \tilde{a} \quad \text{and} \quad (21b)$$

$$A_\alpha = \begin{cases} 1 + \alpha\tilde{l} + \tilde{m} \\ 1 + \alpha\tilde{a} \end{cases} \quad \text{in the case of } \begin{matrix} BM \\ SA \end{matrix} \quad \text{anisotropy,} \quad (21c)$$

we get the dispersion relation for the Rayleigh number R_1 in the form

$$\begin{aligned} & (A_\alpha + i\zeta\sigma_1) \left\{ A [(A + i\sigma_1)(A_\alpha + ip\sigma_1) + Q_1\tilde{m}]^2 + T_1(A + i\sigma_1)^2 \right\} = \\ & = R_1(A - 1)(A + i\sigma_1) \{ (A + i\sigma_1)(A_\alpha + ip\sigma_1) + Q_1\tilde{m} \}. \end{aligned} \quad (22)$$

The dispersion equation (22) for the case of the horizontal magnetic field in y direction is analogous to the vertical magnetic field case of ([3], chap. V).

The transition to dimensionless parameters used in [3, 5, 6] serves here for comparison and checking of complex formulas, but in the following text the numerical results are presented in the space (11) of parameters R , E_z , A , q_z (or $\zeta = 1/q_z$), p ($= R_o/E_z$), and α .

The equation, analogous to the equation (22), in this more "suitable" space of dimensionless parameters has the form,

$$Ra^2 \frac{q_z(K^2 + \lambda)}{(q_z K_\alpha^2 + \lambda)} = \frac{K^2 [E_z(K^2 + \lambda)(K_\alpha^2 + p\lambda) + m^2 \Lambda]^2 + \pi^2 (K^2 + \lambda)^2}{E_z(K^2 + \lambda)(K_\alpha^2 + p\lambda) + m^2 \Lambda}, \quad (23)$$

where, using transforming formulas (21a,b,c),

$$K^2 = a^2 + \pi^2 \quad \text{and} \quad (24a)$$

$$K_\alpha^2 = \begin{cases} \alpha l^2 + m^2 + \pi^2 \\ \alpha a^2 + \pi^2 \end{cases} \quad \text{in the case of } \begin{matrix} BM \\ SA \end{matrix} \text{ anisotropy.} \quad (24b)$$

In recent years, substantial progress has been made in the numerical simulations of dynamos driven by thermal convection studied here. These numerical models are governed by the same dimensionless parameters as those in the problem of rotating magnetoconvection studied here. An important limit for these models of the geodynamo is the limit of neglecting the inertial term $\partial \mathbf{u} / \partial t$, because it is believed that the fast modes are relatively unimportant. The basic dispersion equation in this limit of zero inverse magnetic Prandtl number, $p = \eta / \nu_{zz}$, in the space (11) of dimensionless parameters E_z , A , q_z and α has the form,

$$Ra^2 \frac{q_z(K^2 + \lambda)}{(q_z K_\alpha^2 + \lambda)} = \frac{K^2 [E_z(K^2 + \lambda)K_\alpha^2 + m^2 \Lambda]^2 + \pi^2 (K^2 + \lambda)^2}{E_z(K^2 + \lambda)K_\alpha^2 + m^2 \Lambda}. \quad (25)$$

Meanwhile, we stress that, in the isotropic case $\alpha = 1$, there holds $K_\alpha^2 = K^2$, $q_z = q$, $E_z = E$ and similarly $A_\alpha = A$ and $\mathcal{D}_\alpha = D^2 - a^2$, which are useful for comparing formulas (20 – 25) with the corresponding formulas in [3, 6, 13, 9]. For instance, the relation (25) in the limit $\alpha = 1$ is identical with (3.3) in [13].

4.1 Convection modes in the form of rolls

The main aim of linear stability analysis is to investigate the onset of the convection, thus to find the basic input parameters characterising the system and to find the configuration of instability which starts to convect most easily. The instability may occur if the Rayleigh number, the ratio of destabilising and stabilising forces, reaches a certain critical value. The task is to find the form of perturbation (determined by the wave numbers) which gives the least Rayleigh number for the basic input parameters (Ekman, Elsasser, and Prandtl numbers, and anisotropy parameter). This Rayleigh number is named the critical Rayleigh number and is labeled by R_c . Searching the R_c is related to the process of minimization, but first we must define all investigated modes of convection which compete for the preference in the space of dimensionless parameters (11).

We investigate the onset of steady and overstable convection, which has the form of horizontal rolls and is determined by the two components, l and m , of the horizontal wave vector. The pair, l and m , can be expressed by other pair,

$$a = (l^2 + m^2)^{1/2} \text{ and } \gamma = \tan^{-1}(m/l), \quad (26)$$

where a is the horizontal wave number, and γ is the angle between the axes of rolls and the imposed magnetic field in y direction. Due to (14) the vector (l, m) determines the orientation of convection rolls (rolls are perpendicular to the vector) and in the case of overstable convection this vector determines also the direction of propagating waves.

The case where the wave number l is zero we call cross-rolls, because the rolls are perpendicular to the basic magnetic field. The opposite case is when the wave number m is zero; those modes we call parallel rolls. If both wave numbers are nonzero we call these modes oblique rolls. To investigate the preference means to determine which of these forms of convection is preferred for given E_z , A , q_z , R_o , and α ; see (11). Combining three possible orientations of rolls with steady and overstable convection one can define 5 various modes of convection. Using codes and names by Roberts and Jones [9, 13] we name them P, SC, SO, OC, and OO modes, meaning parallel, steady cross, steady oblique, overstable cross, and overstable oblique rolls, respectively. P modes are never overstable [13].

The minimization process was done in very simple way but sufficient for this problem. Physically relevant part of the two-dimensional space of the wave vector components l and m is covered by a grid. The Rayleigh number is calculated in each point of the grid and the point with the minimal Rayleigh number is found. Suitably chosen surroundings of this point is covered by new grid with higher density of points and again the point with the minimal Rayleigh number is found. The process continues until the desired accuracy is reached with acquiring the R_c and the components l_c and m_c of the critical horizontal wave vector. In the case of overstability formally the same minimization process was used but in each point of the grid the frequency σ was calculated. The σ is the root of the polynomial of the 7th degree which arises from the condition $\text{Im}(R) = 0$ where R corresponds to the expression (23). Obvious root, $\sigma = 0$, is related to the steady convection. The further roots of this equation, related to the overstable convection, stem from the polynomial equation of the 3rd degree for unknown σ^2 . In the cases of more physically possible frequencies than one, the frequency corresponding to the least Rayleigh number is critical frequency, σ_c , as well as the corresponding critical l_c , m_c , and R_c for the overstable mode. Finally, the critical Rayleigh numbers for steady and overstable modes are compared to determine the preferred mode. The determination of the orientation of the preferred modes (including also P modes with $m = 0$ and SC, OC modes with $l = 0$) is a part of the minimization process.

5 Stationary convection, Numerical results

5.1 The ΛE_z regime diagrams

The following numerical results (Fig.2) show the influence of the anisotropy on the distribution of the regions of preference in the ΛE_z -plane, where three regions are coded by the orientation of the preferred rolls

- P \Rightarrow Steady Parallel roll is preferred;
- SC \Rightarrow Steady Cross roll is preferred;
- SO \Rightarrow Steady Oblique roll is preferred.

Figure 2: The regime diagram for steady convection in cases of both type of anisotropy, *SA* and *BM*. Regime diagram shows the regions in the ΛE_z -plane with the preferred type of convection.

Figure 2a shows the influence of *SA* type anisotropy, i.e. *Sa* and *So* on these regions. Solid and dotted lines correspond to the boundaries between individual regions in the anisotropic *Sa* and *So* cases, $\alpha = 0.5$ and $\alpha = 2$, respectively, and dashed lines are the boundaries in the isotropic case, $\alpha = 1$. The boundary between SO and P is shifted to smaller values of the Ekman number E_z in the case of *Sa* anisotropy. It is similar for the boundary between SO and SC, which is shifted to smaller values of the Elsasser number Λ in the *Sa* case. From the physical point of view we can say that *Sa* anisotropy enhances the effect of the Lorentz force, because the same region (region between two oblique lines - boundaries SO-SC), which in the isotropic case is named the weak magnetic field regime, corresponds in the anisotropic *Sa* case to the strong field regime (Λ^* in the isotropic case is greater than the Λ^* in the anisotropic *Sa* case, see the discussion in [13]). Similarly, we can say that *Sa* anisotropy weakens the effect of the Coriolis force, because the region between the two vertical lines, which corresponds to the fast rotation regime in the isotropic case, corresponds to a slower rotation regime in the *Sa* anisotropic case (E_z^* in the isotropic case is greater than E_z^* in the *Sa* anisotropic case).

Figure 2b shows the influence of *BM* type anisotropy on the regime diagram. Solid lines again correspond to boundaries between the various regions for the anisotropic case ($\alpha = 0.5$). The names of the regions are still valid for this *BM* case, even if the boundaries for the isotropic case ($\alpha = 1$) are drawn for comparison by dashed lines in the figure. The boundaries between individual regions of preference are more affected by *BM* anisotropy than by the *SA* anisotropy, even if the parameter of anisotropy is the same. The change of these boundaries is not only quantitative (the boundaries are only shifted in the case of *SA* anisotropy) but the boundaries are changed also qualitatively because their shape is changed. The influence of *BM* anisotropy on the effect of the

Lorentz and Coriolis forces is thus more substantial than in the case of *SA* type anisotropy. Parallel modes can be preferred also in the very fast rotation regime (very small E_z) if the magnetic field is very weak (however, keep in mind that *BM* anisotropy is caused by stronger magnetic fields, see comment to Figure 2c). But only a small increase of the field is sufficient and its effect is considerable. The rolls which are perpendicular to the magnetic field are preferred only in a very narrow region of the Ekman number E_z and the Elsasser number Λ . The distinction between fast rotation regime ($E_z < E_z^*$) and slow rotation regime ($E_z > E_z^*$) is not so simple like in the *SA* anisotropy case and also the isotropic case, because the boundary in the ΛE_z plane between these two regimes is not simply a vertical line given by $E = E_z^*$, i.e. by the number, E_z^* , independently of the Elsasser number, but it is a function of it, i.e. $E_z = E_z(\Lambda)$. It holds so that the greater magnetic field, the greater the value of the boundary Ekman number, E_z^* , which separates the slow rotation regime and the fast rotation regime. The third Figure 2c shows in detail the region of low Ekman and Elsasser numbers, and the region of contact of all three regimes (SC, SO, P). From the figure we can see that in the fast rotation regime arise not only SC modes but also P modes, what could be typical only for *BM* type anisotropy. However, it can not be the case, because *BM* type anisotropy must be caused by stronger magnetic fields, i.e. we must reasonably ignore the smaller Elsasser numbers, e.g. $\Lambda \lesssim 0.01$. Therefore, we focus attention only on SC and SO modes, and not on P modes in all investigated cases of anisotropic diffusive coefficients.

5.2 The critical numbers R_c , a_c , and γ_c

Further numerical results of this stability analysis are presented in Figure 3, which express the dependencies of critical Rayleigh number R_c , critical horizontal wave number a_c , and critical angle of inclination of the rolls γ_c on Elsasser number Λ . The main aim of this paper is to investigate the influence of the anisotropy of diffusive coefficients on the onset of rotating magnetoconvection. Therefore, various curves in the figures correspond to various values of anisotropy parameter α , which is a measure of the anisotropy. For comparison there is also the curve for the isotropic case with $\alpha = 1$ in all figures.

Supposing the following range of input parameters (Elsasser number $\Lambda \in (0.011, 100)$ and Ekman number in the z -direction, $E_z = 3 \cdot 10^{-7}$ ($E_x = \alpha E_z$)) only two types, SC and SO, of orientation of the rolls are possible, because reasonably chosen values of E_z and Λ exclude the preference of P modes (see Fig. 2). The axes of the rolls are either perpendicular to the magnetic field (angle γ_c is equal 90°) or they are inclined to the magnetic field at some nonzero angle. These two cases are distinguished by various types of curves. For mutual comparison of the influence of the anisotropies (Fig. 3) three different values of anisotropy parameters are chosen, $\alpha = 1, 0.5, 0.1$ (for completeness *So* is represented only by one $\alpha = 10$). Various orientations of the rolls are distinguished by the type of the curves, dashed lines for cross rolls, solid lines for oblique rolls in *SA* anisotropy case and dotted lines for oblique rolls in the *BM* anisotropy case. The cross rolls are affected only by *SA* anisotropy, so in the *BM*

Figure 3: Comparison of both types of anisotropy. Dependence of a) critical Rayleigh number R_c , b) critical horizontal wave number a_c and c) critical angle between rolls and basic magnetic field γ_c , on Elsasser number in the case of stratification anisotropy (SA) and anisotropy by Braginsky and Meytlis (BM). Cross rolls — dashed curves, oblique rolls — solid curves (SA), dotted curves (BM).

anisotropy case there is only one line for cross rolls, identical with the isotropic case $\alpha = 1$. If we look at the equations (23, 24b) which are the formulas for the Rayleigh number R , we can see that the anisotropy parameter α is in the BM anisotropy case always multiplied by l^2 — the square of the horizontal wave number l . The horizontal wave number l is zero for rolls perpendicular to the y oriented basic magnetic field. This proves the loss of dependence of the cross rolls properties (e.g. Rayleigh number value) on BM anisotropy. Therefore, we focus our attention on the oblique rolls, i.e. on the solid and dotted lines for the anisotropy parameter values $\alpha = 0.5$ and $\alpha = 0.1$ (and, of course, also to isotropic $\alpha = 1$).

We can see from the Figure 3a, that both BM and Sa facilitate convection by decreasing the critical Rayleigh number R_c (the o type anisotropy, So with $\alpha > 1$, impedes the onset of the convection, because it increases the R_c). Sa anisotropy facilitates convection more effectively than BM anisotropy, because the critical Rayleigh number is smaller in the Sa anisotropy case. This difference is the most evident for $\Lambda = \mathcal{O}(1)$ and decreases for greater values of Λ . The values of Λ for the change of preference (from cross to oblique rolls) are smaller for the BM anisotropy case. The Figure 3b shows, that the difference between critical horizontal wave numbers a_c in the SA case and BM case is small. The critical horizontal wave number is slightly greater in the BM anisotropy case. This difference gradually disappears for the greater values of Λ .

We can see very clearly in the Figure 3c, that the most substantial difference between the influence of the two types of anisotropy on the magnetoconvection is the effect of anisotropies on the boundary value of Λ , for which the transition from cross to oblique rolls occurs. For example, in the case of relatively strong anisotropy ($\alpha = 0.1$) the boundary values of Λ differ by one order of magnitude for the two cases of anisotropy. We can conclude, that the critical angle γ_c is smaller in the BM anisotropy case and the difference between the SA and BM anisotropy cases again disappears for greater values of Λ .

6 Nonstationary convection, Numerical Results

From the geophysical point of view it is more interesting to analyse the influence of anisotropy on the time dependent instabilities. These instabilities are named nonstationary convection (in some papers also overstability). Nonstationary

convection in this model has the form of waves propagating in a certain direction (given by the basic input conditions) to the basic magnetic field (oriented in the y direction), where the angle between the magnetic field and the axes of the rolls is again one of the outputs of this study. The waves are determined by two wave numbers for two horizontal directions x and y and by frequency σ . Both magnetic field and rotation have a stabilizing effect on the fluid, because both can act as restoring forces on displaced fluid parcels and so provide a basis for possible wave motion in the fluid. Therefore, we might expect wave motions to be important in MHD systems such as the Earth's core, stars, the Sun, . . . There are many evidences for wavelike motions from measurements of magnetic field on the surface and from modeling of the field on the CMB. Waves are therefore a natural response of fluid systems to perturbations.

6.1 The Λq_z regime diagrams

In the investigation of nonstationary convection new input parameters, Prandtl numbers, i.e. Roberts number, q , and inverted magnetic Prandtl number, p , appear in the system. Parameter space involves then q and p as well as Λ and E . More precisely, in anisotropy studies⁴ we have p_z , q_z , E_z and α instead of p , q , and E . The regime diagram changes from three-dimensional in the steady case to a more complicated five-dimensional in nonstationary convection. If we want to investigate the influence of anisotropy on the regime diagram of overstable modes in the simplest case, we will consider ideal electrically and thermally conducting and stress free boundaries (as an illustrative case). Further simplification is neglecting of the inertial forces and especially consideration of the often used inviscid approach ($E = 0$). In that case the two-dimensional Λq_z regime diagram is de facto a cross section of the general three-dimensional diagram $\Lambda E_z q_z$ in the plane $E_z = 0$. In the following Figure 4 there are the two Λq_z

Figure 4: Regime diagrams in the cases of both types of anisotropy, a) SA and b) BM . Regime diagrams show the regions in the Λq_z plane with the preferred type of convection in the inviscid case, $E_z = 0$. (The position of symbols SO, SC, OO and OC corresponds to correct regions bounded by solid lines for isotropic case.)

regime diagrams derived numerically. Some important details in the diagrams have been confirmed asymptotically, but we do not present it.

The Figures 4ab show the influence of two anisotropies on this diagram. The curves on these figures represent boundaries between areas with a preferred type of orientation of the rolls. We consider like in [13, 9] four regimes

SC \Rightarrow Steady Cross roll is preferred;

⁴In subsection 3.1 we have already defined (12) anisotropic Prandtl numbers $p = p_z$ and $\zeta = q_z^{-1}$.

- SO \Rightarrow Steady Oblique roll is preferred;
 OC \Rightarrow Overstable Cross roll is preferred;
 OO \Rightarrow Overstable Oblique roll is preferred.

The influence of the stratification anisotropy is described in the Figure 4a. Various types of curves correspond to different cases of *SA* anisotropy (different values of the anisotropy parameter α) and the isotropic case has solid curves. The boundary between the SO and OO regimes is vertical line independent of the Elsasser number Λ and it is in essence a concrete number, $q_z = q_z^*$. This boundary is not an existence boundary of overstable modes, but the boundary of preference. The boundary between the SO and SC regimes is a line, $\Lambda = \Lambda^*(\alpha)$, independent of q_z (steady convection is always independent of the Roberts number), where $\Lambda^*(\alpha)$ is an increasing function of α . This fact was discussed with Fig. 2 for $E_z = 0$ in the case of the ΛE_z regime diagram for steady convection, too. Boundary OO-OC is again a line representing linear dependence $\Lambda = \Lambda(q_z)$ with inclination increasing with α . The remaining boundaries between regimes SO-OC and SC-OC are complicated curves, $\Lambda = \Lambda(q_z)$, and their analytical derivation is also complicated. The main task is to investigate how these boundaries are changed under the influence of the anisotropy of the diffusive coefficients. At first sight one can see that *SA* anisotropy changes the boundaries only quantitatively — the basic nature is preserved. The whole set of boundaries for fixed α is shifted towards the smaller Roberts numbers and greater Λ in the oceanic type anisotropy (*So*, $\alpha > 1$). In the case of atmospheric type (*Sc*, $\alpha < 1$) it is shifted towards the greater Roberts numbers and smaller Λ .

The second Figure 4b describes the influence of *BM* type anisotropy on the regime diagram. Solid lines are related to the isotropic case and the remaining anisotropic cases are distinguished by different types of curves. Comparing with the previous Figure 4a one can see that *BM* anisotropy changes the regime diagram not only quantitatively but even qualitatively. The main difference is related to the SO-OO boundary, which is a simple vertical line $q_z = q_z^*$ independent of the Elsasser number only in the isotropic case. Even weak anisotropy ($\alpha = 0.9$) changes it into the curve $\Lambda = \Lambda(q_z)$. The obliqueness increases with increasing anisotropy. The next important difference from the *SA* case is connected with the OC-OO boundary, which is independent of the anisotropy parameter, the same like the isotropic case. The boundary between SO and SC is similarly a horizontal line like from the *SA* anisotropy case in the previous Figure 4a. However, this similarity of boundaries SO-SC in *SA* and *BM* type anisotropies is not obvious in non-zero E_z cases as is seen in Fig. 2, showing the regime diagram in the ΛE_z -plane for steady convection. The most probable reason is in the well known big difference between the case, $E \rightarrow 0$, and the here considered case, $E = 0$. The remaining boundaries between the regimes SO-OC and SC-OC are again complicated curves $\Lambda = \Lambda(q_z)$ as in *SA* anisotropy.

6.2 The dependence of R_c , a_c , σ_c , and γ_c on Λ

Similarly to the case of steady convection our attention is focused on the influence of anisotropy on the dependencies of the basic parameters of instability (critical Rayleigh number R_c , critical horizontal wave number a_c , critical angle γ_c and critical frequency σ_c) on input parameters describing the basic state (Elsasser number Λ , Ekman number E_z and anisotropy parameter α , but for fixed values of the Prandtl numbers, ζ and p). The following results are presented in the form of figures of dependencies of R_c , a_c , σ_c and γ_c on the Elsasser number for constant Ekman number (or dependencies on the Ekman number with constant Elsasser number), when the inertial forces are considered (non-zero Rossby number). Various strengths of anisotropy are represented by various curves in the figures (curves are labeled by value of the anisotropy parameter α).

Figure 5: The influence of *BM* type anisotropy on nonstationary convection. a) critical angle between rolls and basic magnetic field γ_c and b) critical frequency σ_c as functions of Elsasser number Λ for constant Ekman number $E_z = 3 \cdot 10^{-7}$.

The Figures 5ab show γ_c and σ_c as functions of Λ for the high rotation case, $E_z = 3 \cdot 10^{-7}$, in *BM* type anisotropy (R_c and σ_c are not presented in figures, see comment below.). Seven curves refer to seven various values of the anisotropy parameter $\alpha = 1, 0.7, 0.6, 0.55, 0.5, 0.3, 0.1$. Obviously, at α values, $0 < \alpha < 1$, typical for *BM* anisotropy, it is valid that the smaller anisotropy parameter α , the stronger the anisotropy, i.e. at $\alpha \rightarrow 0$ the *BM* anisotropy is the strongest one, and at $\alpha \rightarrow 1$ is the weakest one. At first sight a considerable effect of the anisotropy is seen in particular in the reduction of the existence interval of Λ in which the instabilities can occur. The interval decreases from the right side and the left side is independent of anisotropy. This means that even strong *BM* anisotropy can not change the fact that overstable modes exist only for sufficiently strong magnetic field (i.e. the Elsasser number has to be large enough; see the left-hand end of the curves). In the first Figure 5a one can see that nonstationary convection starts to exist as cross rolls ($\gamma_c = 90^\circ$) at a certain value of Elsasser number, but for greater values of Λ the rolls are more oblique to the direction of magnetic field. The frequency is independent of the Elsasser number only in the isotropic case, but in anisotropic cases the frequency is a decreasing function of Λ with a sharp drop to zero, which is seen in the Figure 5b. The value of Λ for this sharp drop is an increasing function of the anisotropy parameter α , meaning that this value is smaller for the stronger *BM* type anisotropy. This limitation of overstable modes existence is also evident from the Figure 5a as the sharp right-hand end of the curves. This is one of the important discovered influences of *BM* type anisotropy, because there is no indication for this property in the isotropic case or in *SA* type anisotropy. The critical Rayleigh number R_c and critical horizontal wave number a_c as functions of Λ are not shown, because there is no influence on these dependencies in the

case of *BM* anisotropy for very small $E_z = 3 \cdot 10^{-7}$ as well as in the isotropic case [9, 13]. R_c is not dependent on Λ (and nor α for *OO* - overstable oblique modes), because $R_c = 6\zeta\sqrt{3}\pi^2$ ($\doteq 51.28$ for $\zeta = 0.5$ where ζ is q_z^{-1}). Similarly, the critical horizontal wave number a_c has the same feature. Moreover, $a_c = \pi\sqrt{2} \doteq 4.44$ is constant and even it does not depend on ζ like R_c . There is another reason to not show the dependencies of $R_c(\Lambda)$ and $a_c(\Lambda)$. Varying length curves of these dependencies at different α for *BM* anisotropy overlap and therefore are indistinguishable.

Figure 6: The influence of *BM* type anisotropy on nonstationary convection. a) Critical Rayleigh number R_c , b) critical horizontal wave number a_c , c) critical frequency σ_c and d) critical angle between rolls and basic magnetic field γ_c as functions of Elsasser number Λ for constant Ekman number $E_z = 10^{-3}$.

Next Figure 6 shows the same dependencies (now also including R_c and a_c as functions of Λ) again in the fast rotation case, but now for higher values of the Ekman number $E_z = 10^{-3}$, but for the same Prandtl numbers $p = 0.9$ and $\zeta = 0.5$ like in Fig. 5. Various curves correspond to values of the anisotropy parameter $\alpha = 1, 0.7, 0.6, 0.55, 0.5$, and 0.3 , as for smaller $E_z = 3 \cdot 10^{-7}$ in this *BM* case.

The effect of *BM* anisotropy is obvious from all four Figures 6abcd and the differences between isotropic and anisotropic cases increase more strongly with increasing anisotropy than for the much smaller Ekman number $E_z = 3 \cdot 10^{-7}$ case. Equally as in the preceding case of smaller E_z (Fig. 5) *BM* anisotropy affects non favourably the onset of nonstationary convection from a particular point of view, because it narrows the existence interval of the Elsasser number. From the Figure 6a one can see that the minimal value of Λ for existence of overstability slightly decreases, but the critical Rayleigh number increases for increasing anisotropy. The critical horizontal wave number a_c has similar behaviour; it is a slightly increasing function of *BM* anisotropy. Critical frequencies are decreasing functions of the Elsasser number and have small values. The sharp drop of frequencies and subsequent end of the existence of overstability for higher values of the Elsasser number is seen for all the considered values of the anisotropy parameter α . The value of Λ at which the sharp drop of frequency occurs is a decreasing function of *BM* anisotropy (the smaller anisotropy parameter α , the smaller Λ).

The same dependencies were investigated also in the case of stratification anisotropy. The influence of this *SA* type anisotropy on nonstationary convection is very simple and therefore is not presented in figures. The critical Rayleigh number R_c as well as the critical horizontal wave number a_c are not influenced by *SA* type anisotropy and have the same value as in the isotropic case [9, 13] ($R_c = 6\zeta\sqrt{3}\pi^2$ where ζ is q_z^{-1} and $a_c = \pi\sqrt{2} \doteq 4.44$). Both critical numbers together with the critical frequency σ_c are independent of the Elsasser number Λ . The critical frequency is a decreasing function of *Sa* type anisotropy, as in

the case of *BM* type anisotropy. Thus the smaller the anisotropy parameter α , the smaller the critical frequency σ_c .

6.3 The dependence of R_c , a_c , σ_c , and γ_c on E_z

Figure 7: The influence of *BM* type anisotropy on nonstationary convection. a) Critical Rayleigh number R_c , b) critical horizontal wave number a_c , c) critical frequency σ_c and d) angle between rolls and basic magnetic field γ_c as functions of Ekman number E_z for constant Elsasser number $\Lambda = 3$.

The next Fig. 7 is again related to the *BM* case, but shows R_c , a_c , σ_c and γ_c as functions of the Ekman number E_z for the constant Elsasser number $\Lambda = 3$. The Prandtl numbers $p = 0.9$ and $\zeta = 0.5$ are the same like in other nonstationary studies presented in Figures 5 and 6.

The critical Rayleigh number R_c is for smaller Ekman number E_z not dependent on it and is not influenced by *BM* anisotropy. The slight dependence of R_c on E_z and α is only for the greater $E_z > \mathcal{O}(10^{-5})$. For smaller Ekman numbers the critical horizontal wave number is not influenced either by the anisotropy or by the Ekman number alone. However, for Ekman numbers greater than $E_z = \mathcal{O}(10^{-5})$ the influence of anisotropy starts to be evident and the horizontal wave number behaves as an increasing function of the Ekman number for the case of strong anisotropy ($\alpha = 0.01$) as well as a decreasing function of the Ekman number for weak anisotropy up to the isotropic case ($\alpha = 1$), with a smooth transition between these two behaviours. We can see similar behaviour in the Figure 7d where the critical angle γ_c is a function of anisotropy but independent of the Ekman number for small Ekman numbers. For greater E_z the dependence on E_z itself appears and the effect of *BM* anisotropy is also qualitative. In the isotropic case the angle γ_c increases with increasing Ekman number so the rolls tilt into the direction perpendicular to the magnetic field. *BM* anisotropy changes this behaviour into the opposite one — for greater Ekman numbers the rolls tilt into the direction parallel to the magnetic field (the angle γ_c decreases). The third Figure 7c shows that sharp drop of frequency occurs for the cases of stronger anisotropy, the nonstationary convection does not exist for values of the Ekman number greater than the value at which the frequency reaches zero (this value is an increasing function of the anisotropy parameter α). The *BM* type anisotropy handicaps the overstability by reducing the range of Ekman numbers at which the overstability exists (similar to the case of the Elsasser number).

7 Conclusions

The influence of anisotropy of the diffusion coefficients (thermal diffusion and viscosity) on the marginal stability of a horizontal planar layer of electrically conducting fluid has been studied. The layer is permeated by a horizontal homogeneous magnetic field and rotates about a vertical axis of rotation. This model was employed by Roberts and Jones [13, 9] and also by Eltayeb [5, 6]. Considering yet the isotropic diffusion we advanced these studies by including two types of anisotropic diffusive coefficients, *SA* — stratification anisotropy ($\nu_{zz} \neq \nu_{xx} = \nu_{yy}$, $\kappa_{zz} \neq \kappa_{xx} = \kappa_{yy}$) and *BM* — the anisotropy of Braginsky and Meytlis [1] ($\nu_{zz} = \nu_{yy} > \nu_{xx}$, $\kappa_{zz} = \kappa_{yy} > \kappa_{xx}$).

Three regimes, as in [13, 9, 5, 6], are possible in the case of steady convection: P – rolls parallel to the magnetic field; SO – oblique rolls; and SC – cross rolls. Both types of anisotropy influence the ΛE_z regime diagram (Fig. 2). The boundaries between individual regions of preference are more affected by *BM* anisotropy than by *SA* anisotropy in comparison with the isotropic case. *SA* anisotropy of atmospheric type enhances the effect of the Lorentz force and weakens the effect of the Coriolis force. In *BM* anisotropy the change of these boundaries is not only quantitative (the boundaries are only shifted in the *SA* anisotropy case), but the boundaries are changed also qualitatively because their shape is changed. The influence of *BM* anisotropy on the effect of the Lorentz and Coriolis forces is thus more substantial than in the *SA* anisotropy case. *SA* anisotropy of atmospheric type facilitates convection more effectively than *BM* anisotropy, because the critical Rayleigh number is smaller in this *SA* case. Critical horizontal wave numbers are slightly greater in the *BM* anisotropy case than in the *SA* and isotropic cases. The differences between the influence of *SA* and *BM* anisotropy are the most evident for $\Lambda = \mathcal{O}(1)$ and decrease for greater values of Λ .

Supposing nonstationary convection new input parameters appear. Neglecting inertial forces and considering an inviscid approach the influence of both types of anisotropy on the Λq_z regime diagram has been studied. Four regimes are compared, as in [13, 9, 5, 6]: steady cross rolls (SC); steady oblique rolls (SO); overstable cross rolls (OC), and overstable oblique rolls (OO). *SA* anisotropy changes the boundaries between regimes only quantitatively — the basic nature is preserved (in comparison with the isotropic case [13]). The region boundaries are shifted towards the smaller Roberts numbers and greater Elsasser numbers in the case of oceanic type anisotropy ($\alpha > 1$), and in atmospheric type ($\alpha < 1$) they are shifted in opposite directions. *BM* anisotropy changes the regime diagram not only quantitatively but even qualitatively. In *BM* anisotropy the OC-OO boundary is independent of the anisotropy parameter and is the same as for the isotropic case.

The influence of anisotropies on critical numbers (R_c, a_c, γ_c and σ_c) as functions of the Elsasser number Λ and the Ekman number E_z has been also investigated. In the case of very small $E_z = 3 \cdot 10^{-7}$ the critical Rayleigh number R_c is not dependent on Λ (and nor α for OO - overstable oblique modes), because $R_c = 6\zeta\sqrt{3}\pi^2$ ($\doteq 51.28$ for $\zeta = 0.5$). Similarly, the critical horizontal wave num-

ber a_c has the same feature. Moreover, $a_c = \pi\sqrt{2} \doteq 4.44$ is constant. These features hold for both anisotropies. It means, that anisotropy does not change the preference of the overstable modes in the very small $E_z = 3 \cdot 10^{-7}$ case.

The effect of *BM* anisotropy is more substantial for larger Ekman number $E_z = 10^{-3}$ (Fig. 6). The difference between the isotropic and anisotropic *BM* cases increases more strongly with increasing anisotropy than for the much smaller Ekman number $E_z = 3 \cdot 10^{-7}$ case. R_c and a_c are no longer simple constants, but both are functions of Λ and the anisotropy parameter α .

There is one unique property of *BM* anisotropy (in comparison with the *SA* or/and isotropic cases). *BM* anisotropy handicaps the overstability by reducing the ranges of the Elsasser number as well as the Ekman number at which overstability occurs (see e.g. drops of frequencies in Figs 5 - 7 in curves $\sigma_c(\Lambda)$ and $\sigma_c(E_z)$). This reduction is in the sense that greater the *BM* anisotropy, the smaller the maximum Λ and E_z at which nonstationary convection ceases to occur.

We expect that additional study (in preparation) of anisotropic diffusivities influence on rotating magnetoconvection matched to equatorial regions will reveal other interesting facts.

Acknowledgements

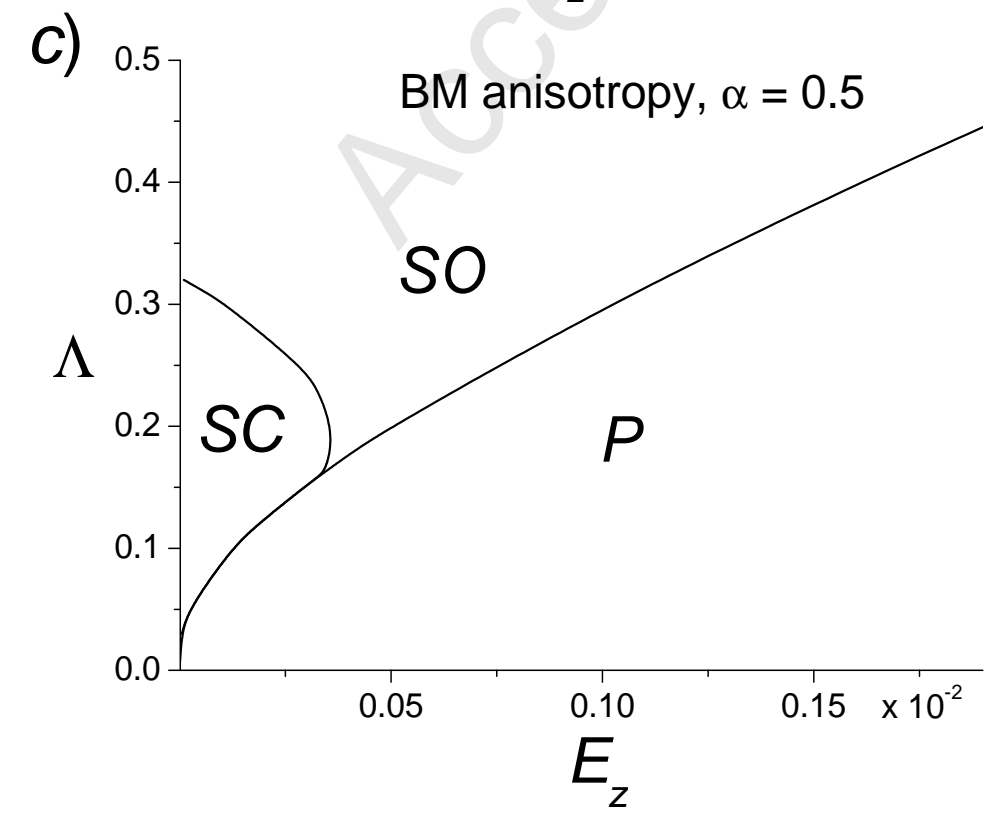
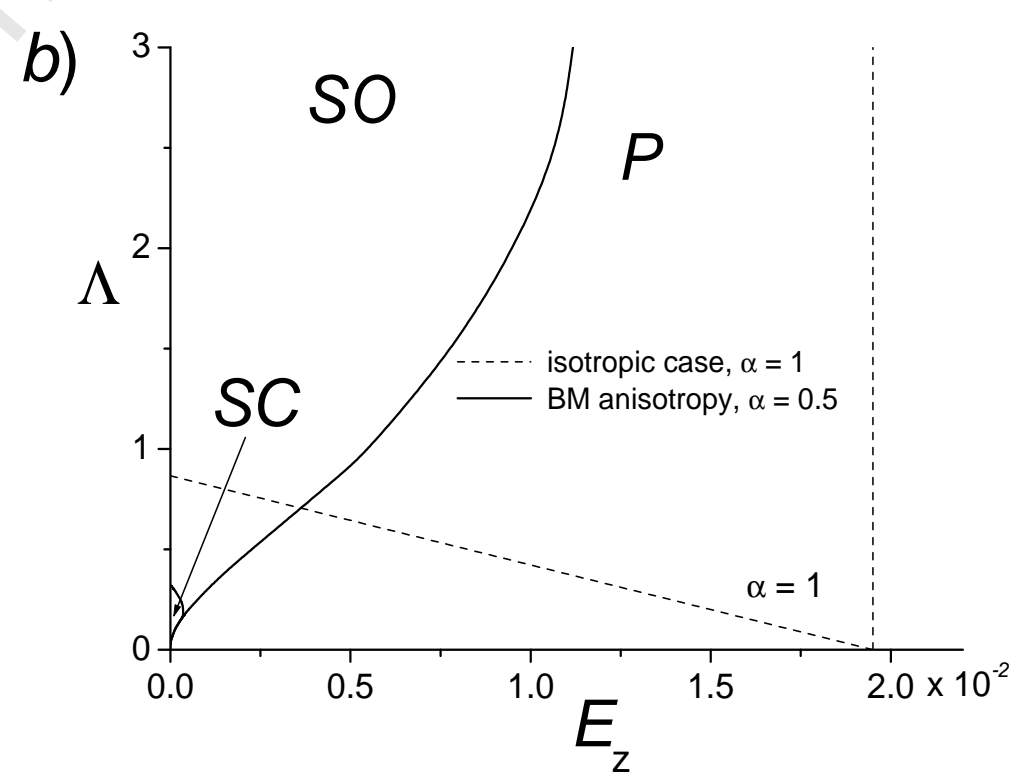
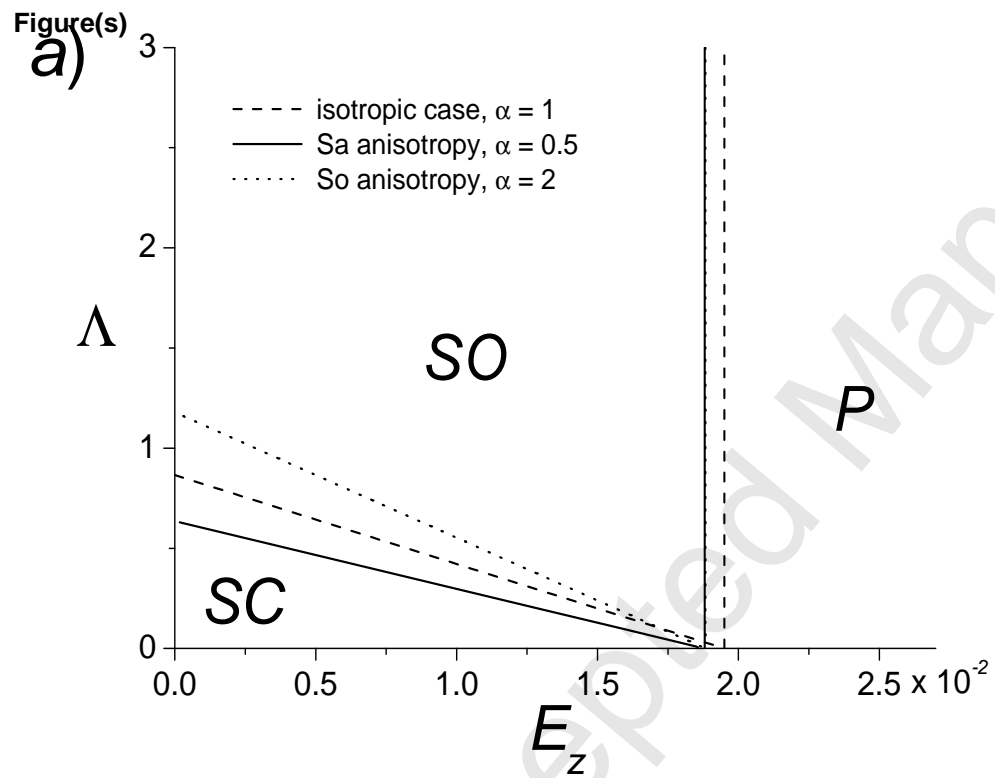
This work was supported by scientific grant agency VEGA (grant n. 1/3069/06) and by Comenius University (grant n. UK /398/2008). We are also grateful to Sebastián Ševčík and Alexandra Marsenić for helpful discussions and hints. We would like to thank also to the organizers of SEDI meeting in Kunming for financial support to present our results by TS. We are also happy to express our gratitude to both unknown reviewers for very important comments and helpful hints, which has helped us to revise our manuscript to be more clear and readable.

References

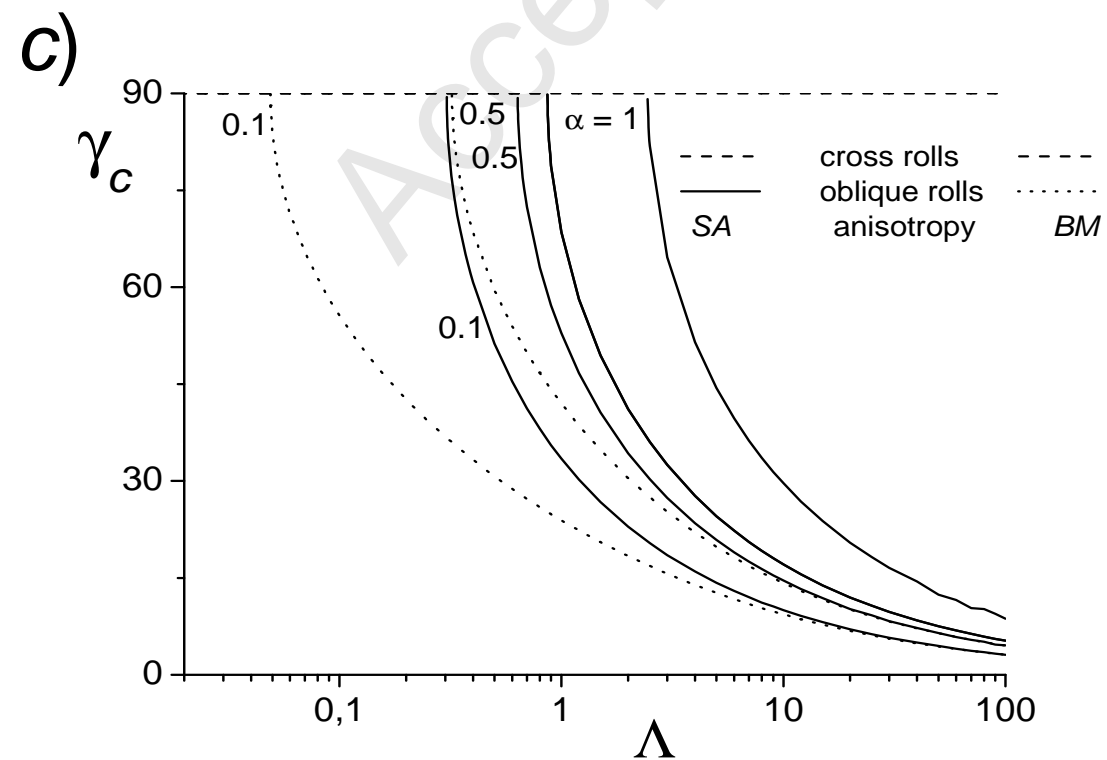
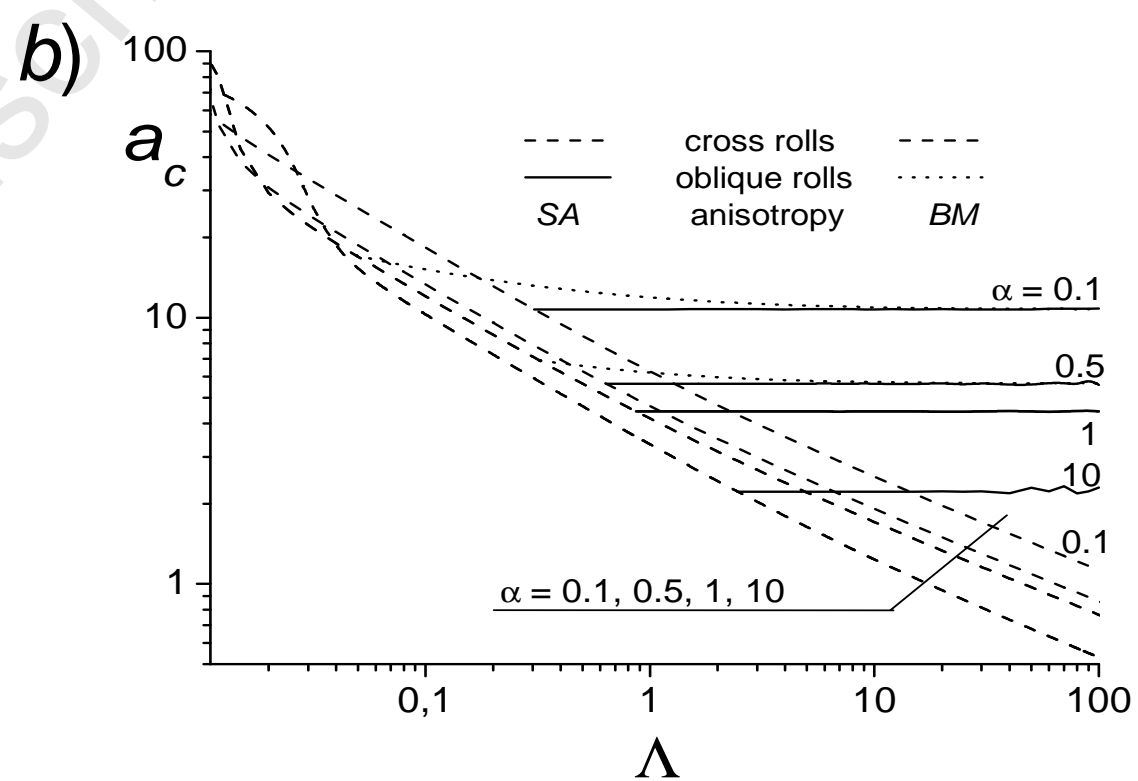
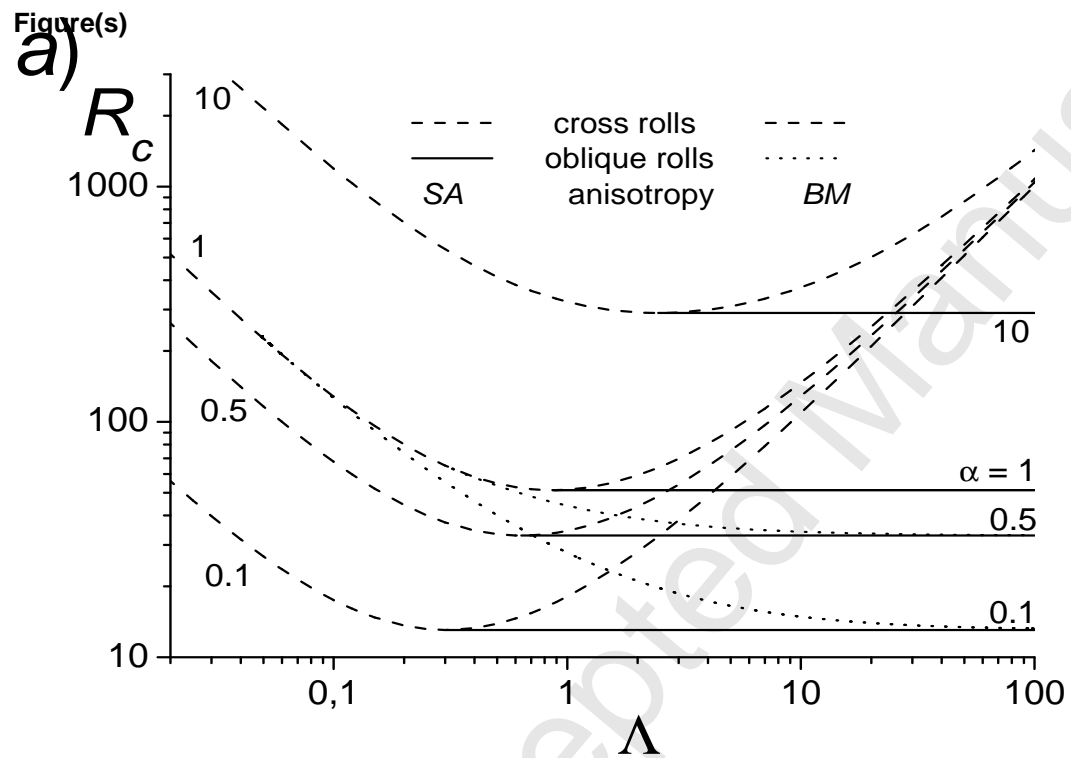
- [1] Braginsky, S. I., Meytlis, V. P., 1990. Local turbulence in the Earth's core. *Geophys. Astrophys. Fluid Dynamics* 55, 71–87.
- [2] Brestenský, J., Šoltis, T., Ševčík, S., 2005. Linear Rotating Magnetoconvection with anisotropic diffusive coefficients. In: *Proceedings of the Riga Pamiir conference, Fundamental and Applied MHD* 1, 101–104.
- [3] Chandrasekhar, S., 1961. *Hydrodynamic and hydromagnetic stability*. Clarendon Press, Oxford.
- [4] Donald, J.T., Roberts, P.H., 2004. The effect of Anisotropic heat transport in the Earth's core on the Geodynamo. *Geophys. Astrophys. Fluid Dynam.* 98, 367–384.
- [5] Eltayeb, I.A., 1972. Hydromagnetic convection in a rapidly rotating fluid layer. *Proc. R. Soc. Lond. A* 326, 229–254.

- [6] Eltayeb, I.A., 1975. Overstable hydromagnetic convection in a rapidly rotating fluid layer. *J. Fluid Mech.* 71, 161–179.
- [7] Fearn, D., Roberts, P.H., 2007. The geodynamo, Chapter 4. In: Dormy, E., Soward, A.M. *Mathematical Aspects of Natural Dynamos*. Taylor and Francis.
- [8] Gubbins, D., Herrero-Bervera, E., 2007. *Encyclopedia of Geomagnetism and Paleomagnetism*. Springer.
- [9] Jones, C.A., Roberts, P.H., 2000. The Onset of Magnetoconvection at Large Prandtl Number in a Rotating Layer II. Small Magnetic Diffusion. *Geophys. Astrophys. Fluid Dynam.* 93, 173–226.
- [10] Matsushima, M., Nakajama, T., Roberts, P.H., 1999. The anisotropy of local turbulence in the Earth's core. *Earth Planet Space* 51, 277–286.
- [11] Phillips, C.G., Ivers, D.J., 2000. Spherical anisotropic diffusion models for the Earth's core. *Phys. Earth Planet. Inter.* 117, 209–223.
- [12] Phillips, C.G., Ivers, D.J., 2001. Spectral interactions of rapidly anisotropic turbulent viscous and thermal diffusion in the Earth's core. *Phys. Earth Planet. Inter.* 128, 93–107.
- [13] Roberts, P.H., Jones, C.A., 2000. The Onset of Magnetoconvection at Large Prandtl Number in a Rotating Layer I. Finite Magnetic Diffusion. *Geophys. Astrophys. Fluid Dynam.* 92, 289–325.
- [14] Schubert, G., 2007. *Treatise on Geophysics, Volume 5 – Geomagnetism*, ed. Kono, M., *Volume 8 – Core Dynamics*, ed. Olson, P., Elsevier.
- [15] Šimkanin, J., Brestenský, J., Ševčík, S., 2003. Problem of the rotating magnetoconvection in variously stratified fluid layer revisited. *Studia Geophys. Geod.* 47, 827–845.
- [16] Šoltis, T., 2008. Rotating magnetoconvection at various types of anisotropic diffusion coefficients. Doctor, RNDr, thesis, FMPI, Comenius University, Bratislava, in Slovak.
- [17] Soward, A. M., 1979. Thermal and magnetically driven convection in a rapidly rotating fluid layer. *J. Fluid Mech.* 90, 669–684.

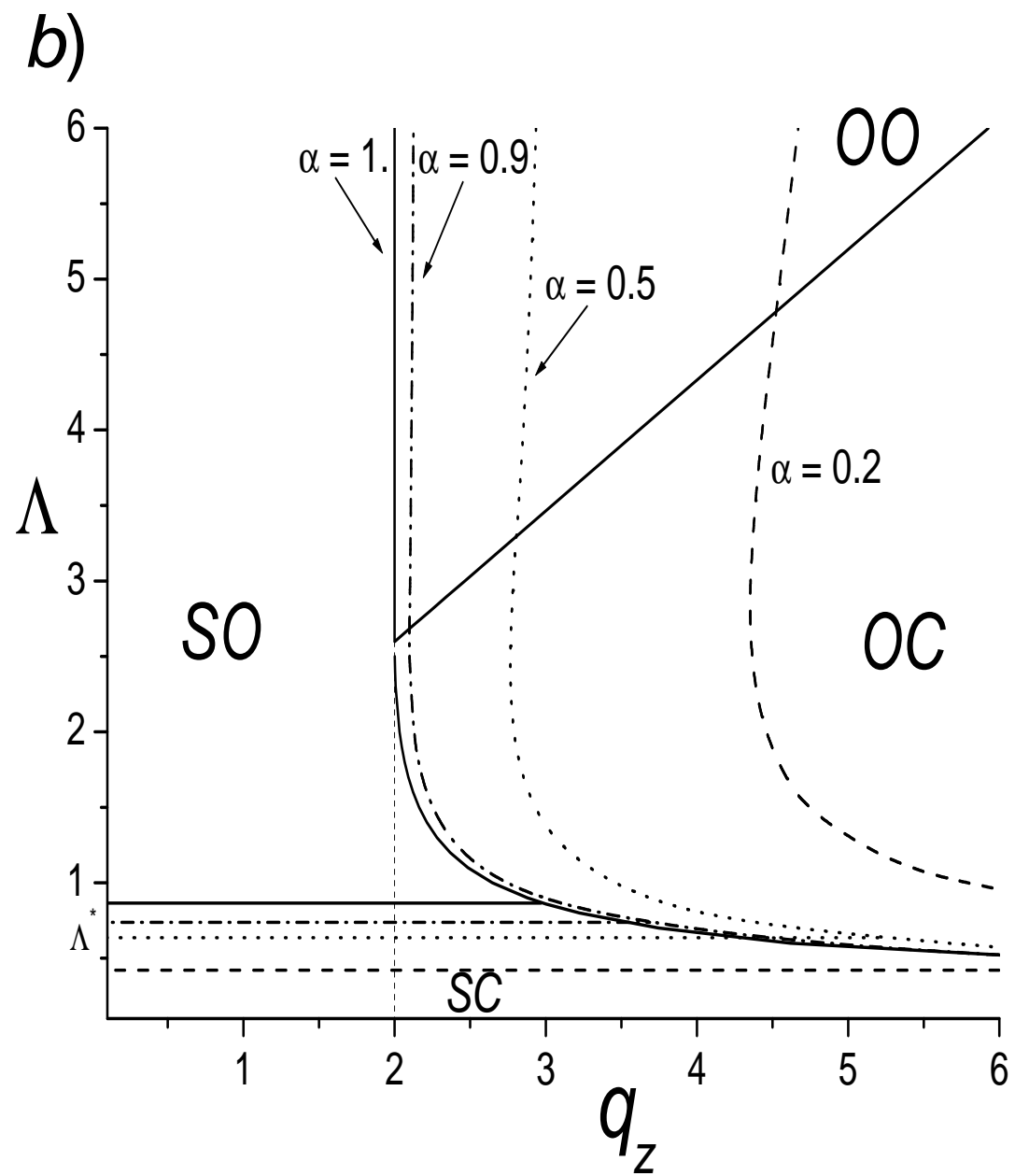
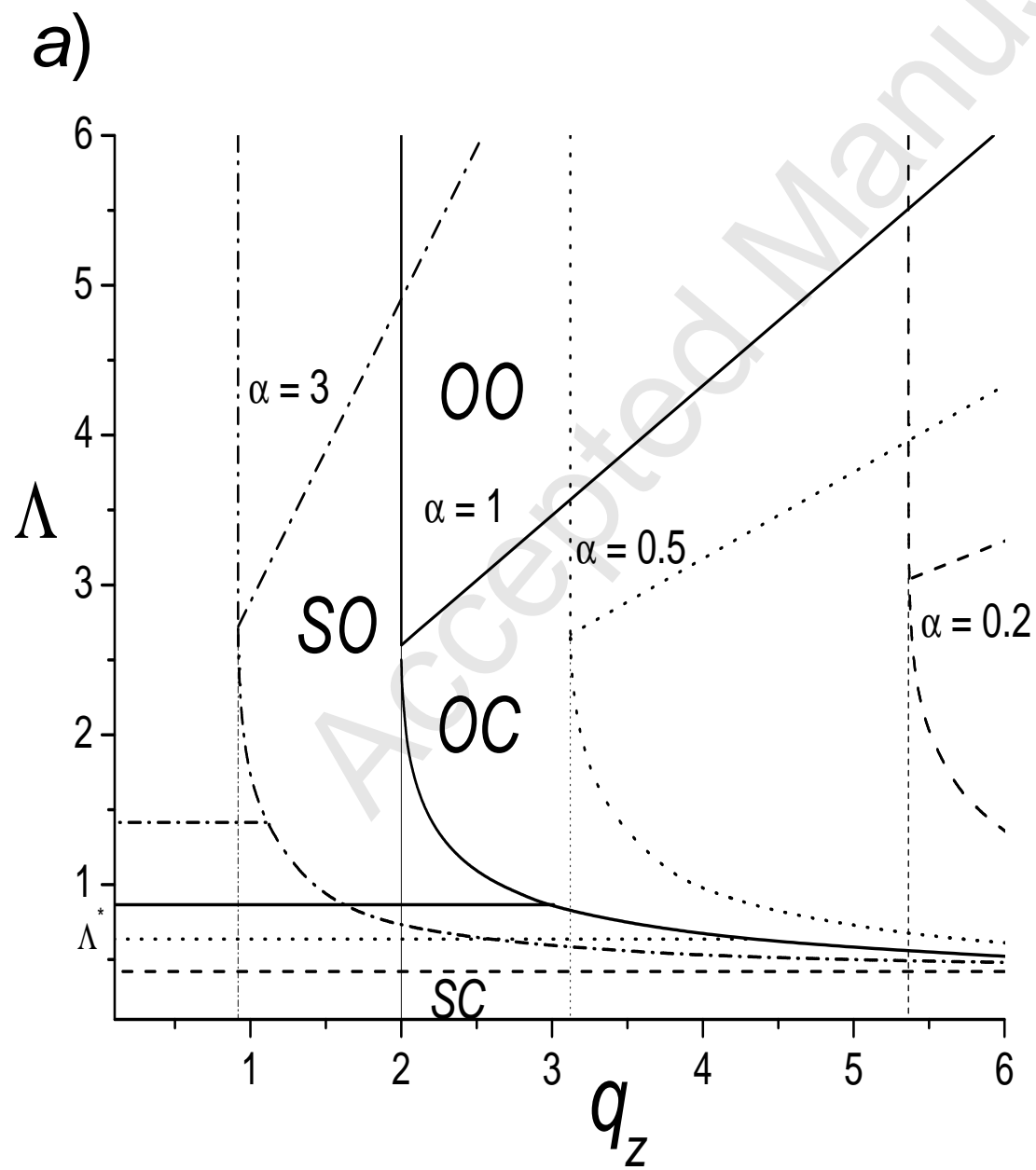
Figure(s)

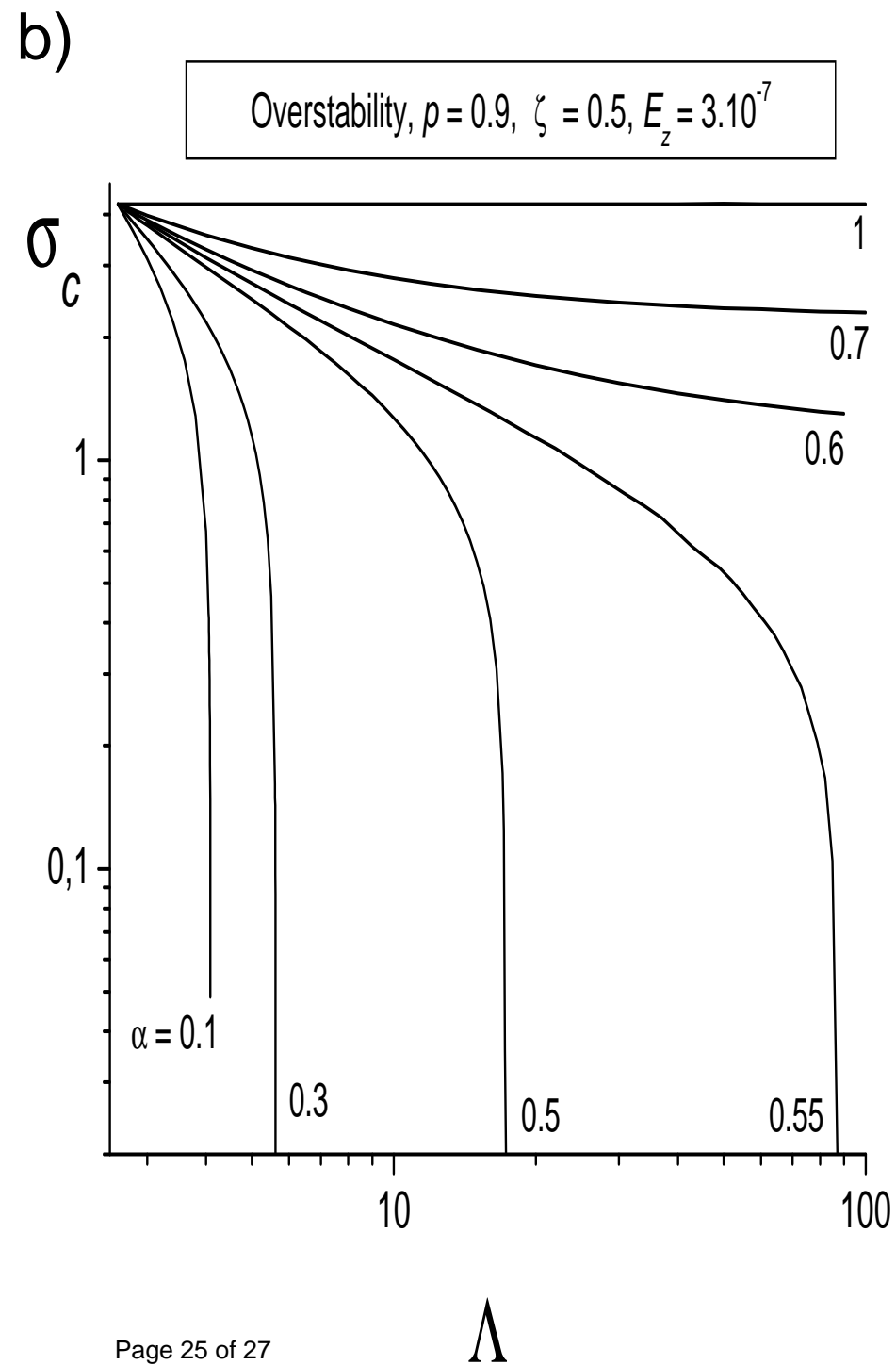
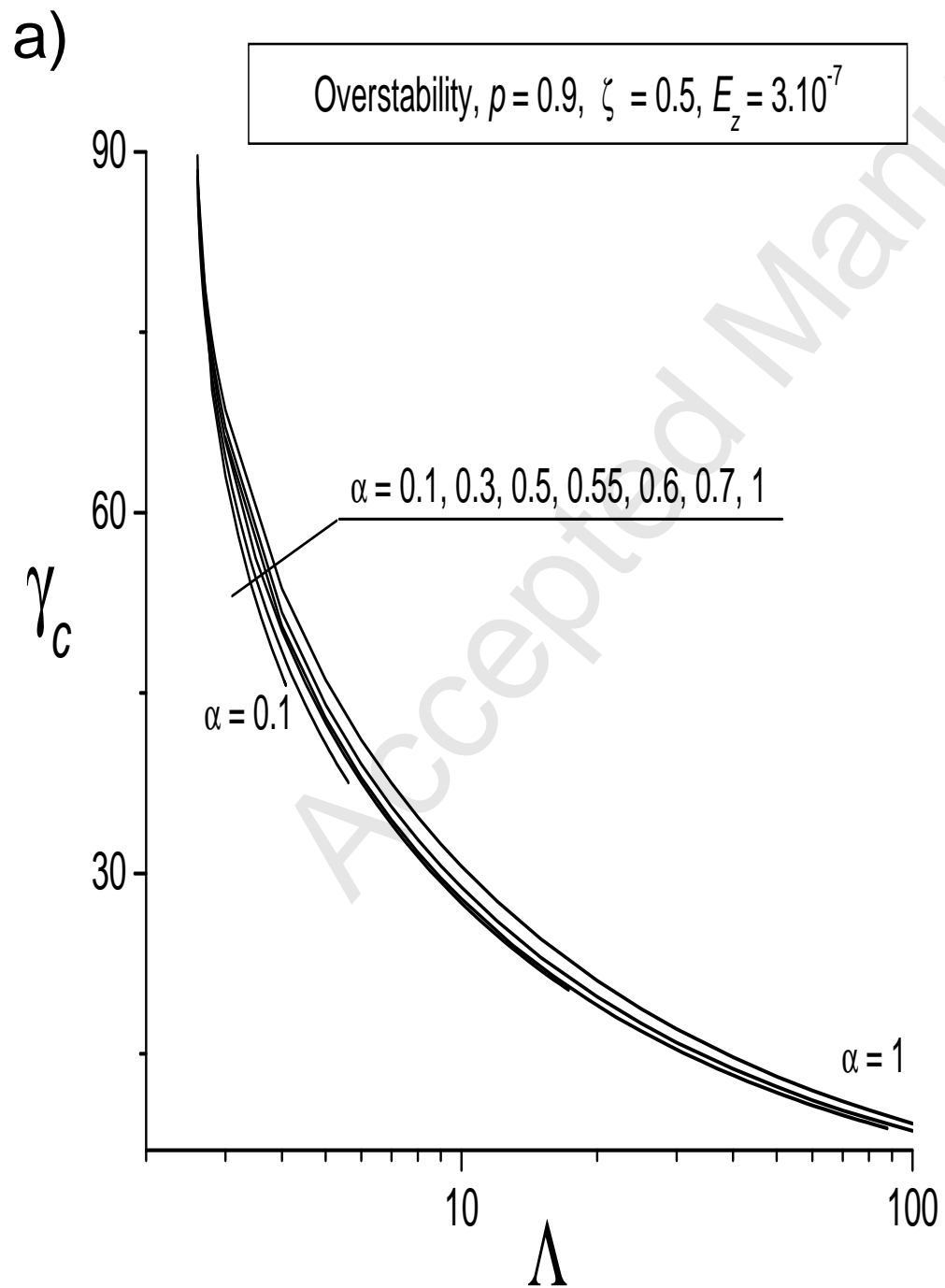


Figure(s)

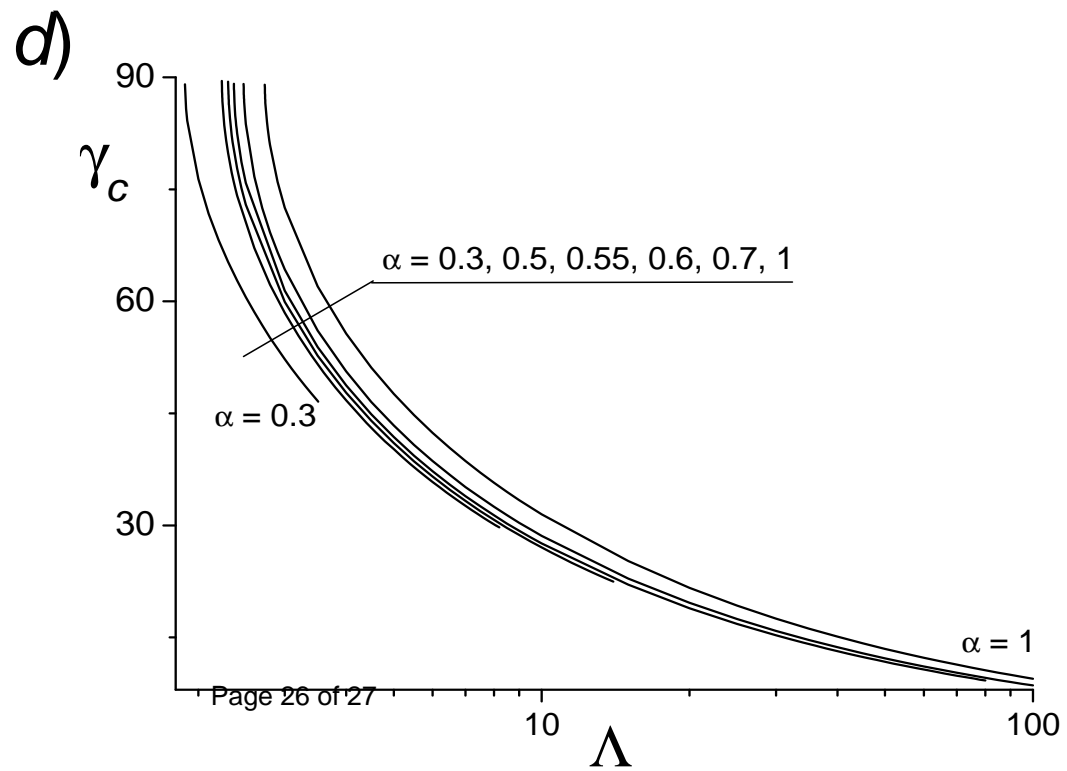
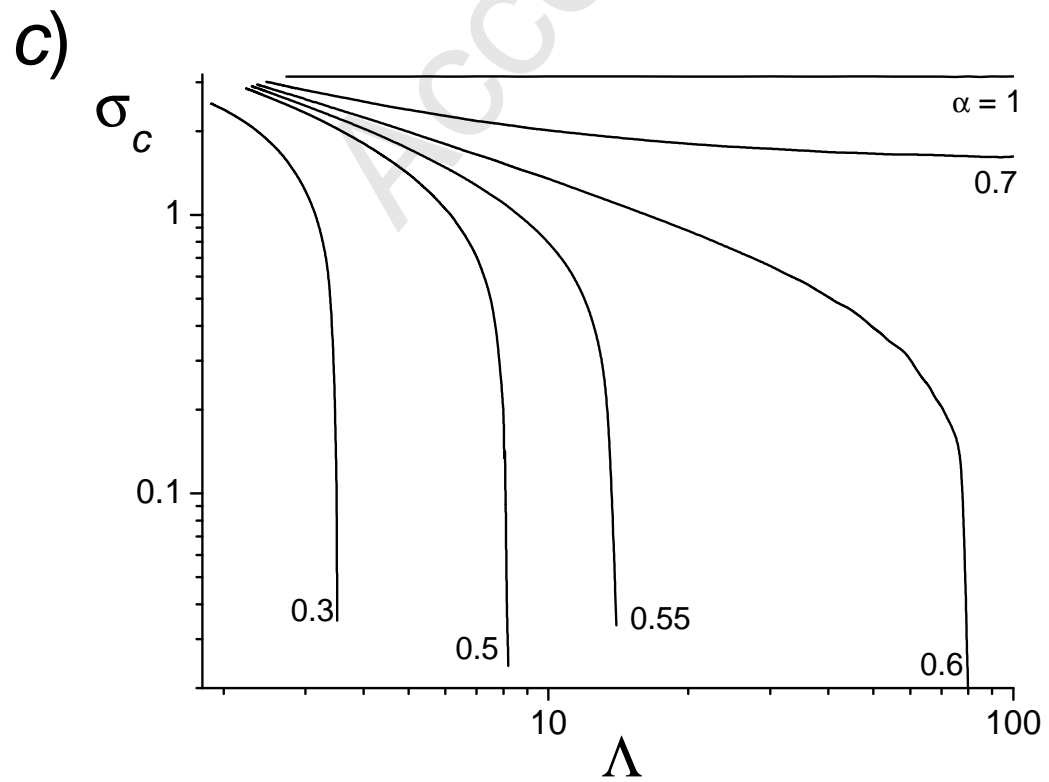
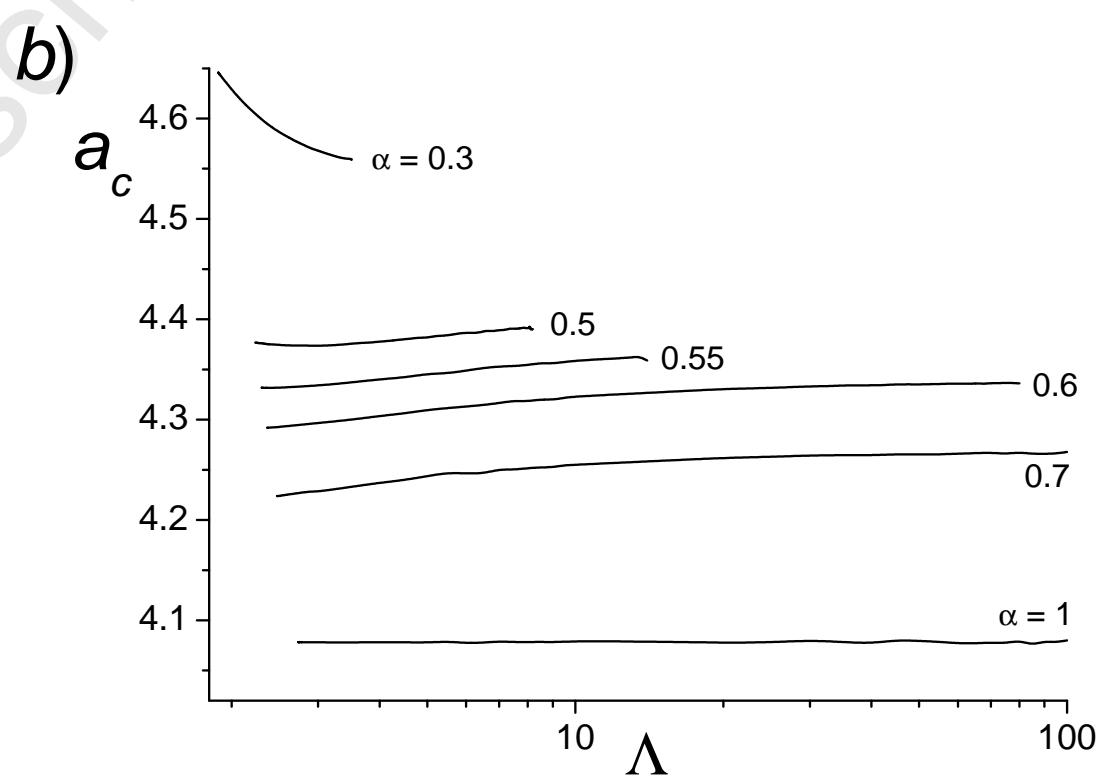
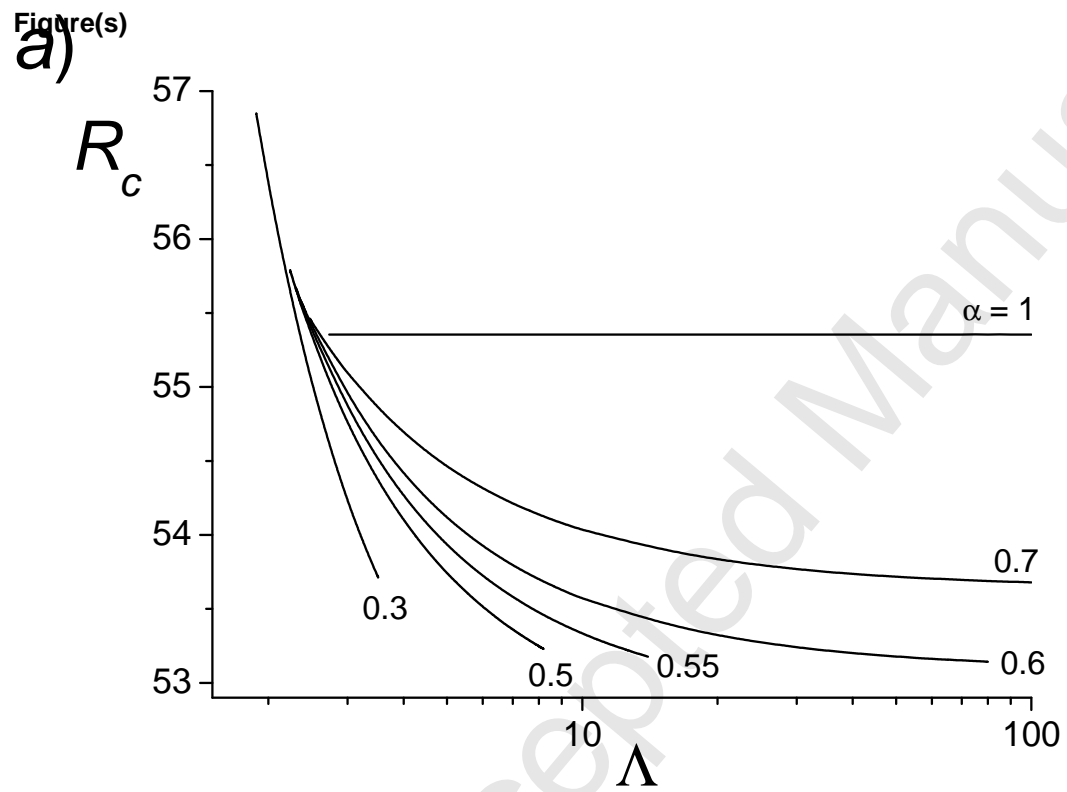


SA / BM





Figure(s)



Figure(s)

